CELL STRUCTURE AND FUNCTION 36: 13–20 (2011)

Rapid Communication

Radiation-induced Cancer Cell Repopulation: A Possible Mechanism Implied by Experiments Using Transplantable Mouse-derived Sarcoma Cell Line

Takeshi Nishioka[1*], Motoaki Yasuda[2], Tsuguhide Takeshima[3], Hisashi Haga[4], Yusuke Miyai[4], Ken-ichiro Shibata[2], Rie Yamazaki[1], Hiroki Shirato[3], Masahiro Teduka[5], and Hiroyuki Date[1]

[1]*Department of Biomedical Sciences and Engineering, Faculty of Health Science, Hokkaido University, N12-W5, Kita-ku, Sapporo 060-0812, Japan,* [2]*Department of Oral Pathological Sciences, Graduate School of Medicine, Hokkaido University, N13-W7, Kita-ku, Sapporo 060-8586, Japan,* [3]*Department of Radiology, Hokkaido University Graduate School of Medicine, N15-W7, Kita-ku, Sapporo 060-8638, Japan,* [4]*Transdisciplinary Life Science Course, Faculty of Advanced Life Science, Hokkaido University, N10-W8, Kita-ku, Sapporo 060-0810, Japan,* [5]*Resources and Energy Department, Hokkaido Industrial Research Institute, N19W11, Kita-ku, Sapporo 060-0819, Japan*

ABSTRACT. **Purpose: Treatment with any cytotoxic agent can trigger surviving cells in a tumor to divide faster than before. This phenomenon is widely recognized as "repopulation". To better clarify the mechanism, gene expression profiling and pathological experiments were performed. Materials and Methods: A mouse fibrosarcoma cell line, QRsP, was used. Cells were irradiated with 10 Gy. Colony assay and cloning were performed. Six clones were established. cDNA analysis was performed on the clone that showed the largest number of colonies on the 2nd 10 Gy irradiation. Mouse transplantation experiment was then carried out. Results: cDNA analysis showed that cyclin-dependent kinase inhibitors, p16 and p57 were down-regulated; 14.8- and 12.0-fold, respectively for the tolerant clone. Matrix metalloproteinase 3 and 13 were up-regulated; 22.5- and 25.8-fold, respectively. Transplantation ratio was 100% (5/5) for the tolerant clone whereas it was 40% (2/5) for the parent. Under light microscope, the mean mitotic cell number was 4.0+/–3.9 for the parent, and 12.8+/–3.4 for the tolerant clone ($p<0.01$, Student's *t*-test). Conclusions: This study implies that repopulation is not a temporary reaction to irradiation. It is caused probably by "clonal" gene-expression changes, though it remains unknown whether the changes are attributable to tolerant cell selection or to gene mutation/modification.**

Key words: p16/radiotherapy/irradiation/repopulation/matrix metalloproteinase

Introduction

Radiotherapy is one of the most effective treatments for various malignancies. It can cure tumors arising in the head and neck, uterine cervix, and recently even the lung (Inoue *et al.*, 2009). It also plays an important role (combined with surgery or chemotherapy) in the management of breast cancer and lung cancer; both are now leading causes of death worldwide. Several attempts have been made to increase the tumor-killing effects of radiotherapy. Among them, shortening the overall treatment time of radiotherapy to counterattack tumor repopulation has been the focus of attention for the past decade. Recently, molecular-targeted medicines have been shown to be effective. Repopulation or regeneration is a widely recognized phenomenon in which treatment with any cytotoxic agent can trigger surviving cells in a tumor to divide faster than before (Kim and Tannock, 2005).

Recent reports on the use of accelerated irradiation regimens are encouraging, but inevitably accompanied by increased toxicities (Bernier, 2005). Achieving a high degree of tumor control with fewer complications is a difficult proposition, which makes it necessary to understand tumor behavior during radiotherapy at the genetic and molecular levels. Despite widespread awareness of tumor regeneration among oncologists and biologists, little is known about its basic mechanism. Why and how do tumor cells survive irradiation and start to regenerate?

*To whom correspondence should be addressed: Takeshi Nishioka, Department of Biomedical Sciences and Engineering, Faculty of Health Sciences, Hokkaido University, N12-W5, Kita-ku, Sapporo 060-0812, Japan.
Tel/Fax: +81–11–706–3411
E-mail: trout@hs.hokudai.ac.jp

Table I.

	Gene Name	Description	Fold Change
(a) Up-regulated genes *in vitro*			
1	NM_031168	interleukin 6 (Il6), mRNA	36.0
2	NM_008607	matrix metalloproteinase 13 (Mmp13), mRNA	25.8
3	NM_011315	serum amyloid A 3 (Saa3), mRNA	24.8
4	NM_010809	matrix metalloproteinase 3 (Mmp3), mRNA	22.5
5	BC020275	NEUTROPHIL GELATINASE-ASSOCIATED LIPOCALIN PRECURSOR (NGAL) (P25) (SV-40 INDUCED 24P3 PROTEIN) (LIPOCALIN 2)	15.6
6	NM_008176	GRO1 oncogene (Gro1), mRNA	12.8
7	K02782	Mouse complement component C3 mRNA, alpha and beta subunits, complete cds	9.0
8	NM_009117	serum amyloid A 1 (Saa1), mRNA	9.8
9	NM_011198	prostaglandin-endoperoxide synthase 2 (Ptgs2), mRNA	8.5
10	NM_007428	angiotensinogen (Agt), mRNA	7.8
11	NM_009705	arginase type II (Arg2), mRNA	6.2
12	NM_011337	small inducible cytokine A3 (Scya3), mRNA	6.1
13	NM_007825	cytochrome P450, 7b1 (Cyp7b1), mRNA	5.4
14	AK013991	unknown EST	5.4
15	NM_007679	CCAAT/enhancer binding protein (C/EBP), delta (Cebpd), mRNA	5.4
16	NM_009378	thrombomodulin (Thbd), mRNA	5.3
17	NM_010884	N-myc downstream regulated 1 (Ndr1), mRNA	5.2
18	D26157	Mouse prostacyclin receptor mRNA	5.0
19	NM_010330	embigin (Emb), mRNA	5.0
20	NM_133662	immediate early response 3 (Ier3), mRNA	4.9
21	AK002567	METALLOTHIONEIN-II (MT-II) homolog [ ]	4.9
22	BC010816	Similar to hypothetical protein FLJ10044, clone MGC:19129 IMAGE:4212305, mRNA, complete cds	4.9
23	NM_010728	lysyl oxidase (Lox), mRNA	4.8
24	NM_007762	corticotropin releasing hormone receptor (Crhr), mRNA	4.6
25	NM_133775	RIKEN cDNA 9230117N10 gene (9230117N10Rik), mRNA	4.5
26	NM_013473	annexin A8 (Anxa8), mRNA	4.2
27	AK018504	unknown EST	4.2
28	NM_030612	molecule possessing ankyrin-repeats induced by lipopolysaccharide (Mail-pending), mRNA	4.2
29	NM_009061	regulator of G-protein signaling 2 (Rgs2), mRNA	4.2
30	NM_013473	annexin A8 (Anxa8), mRNA	4.2
(b) Down-regulated genes *in vitro*			
1	AK032881	mesoderm specific transcript	23.1
2	AB041591	brain cDNA, clone MNCb-2717	16.2
3	AK046674	9130002C22RIK PROTEIN homolog [Mus musculus]	15.6
4	NM_009877	cyclin-dependent kinase inhibitor 2A (Cdkn2a), mRNA	14.8
5	NM_021792	interferon-inducible GTPase (Iigp-pending), mRNA	13.9
6	M55219	Mouse HSR mRNA, clone pMmHSRc-[1,3,3E,10 and 10E]	13.4
7	NM_009876	cyclin-dependent kinase inhibitor 1C (P57) (Cdkn1c), mRNA	12.0
8	NM_010514	insulin-like growth factor 2 (Igf2), mRNA	9.9
9	NM_008357	interleukin 15 (Il15), mRNA	8.9
10	NM_020577	methyltransferase Cyt19 (Cyt19-pending), mRNA	8.5
11	AK005747	RIKEN cDNA 1700007P19 gene	8.0
12	NM_010052	delta-like 1 homolog (Drosophila) (Dlk1), mRNA	7.7
13	Y15910	mRNA for dia protein	7.4
14	AK008273	rho, GDP dissociation inhibitor (GDI) beta	6.7
15	NM_018857	mesothelin (Msln), mRNA	6.6
16	NM_133654	CD34 antigen (Cd34), mRNA	6.6
17	AK080076	unknown EST	6.5
18	NM_011920	ATP-binding cassette, sub-family G (WHITE), member 2 (Abcg2), mRNA	6.5
19	NM_053152.1	killer cell lectin-like receptor subfamily A, member 22 (Klra22), mRNA	6.3
20	BC013672	Similar to hypothetical protein FLJ20035, clone MGC:19297 IMAGE:4037887, mRNA, complete cds	6.3
21	NM_019440	interferon-g induced GTPase (Gtpi-pending), mRNA	6.0
22	NM_019955	receptor-interacting serine-threonine kinase 3 (Ripk3), mRNA	5.7
23	NM_025582	RIKEN cDNA 2810405K02 gene (2810405K02Rik), mRNA	5.7
24	NM_011909	ubiquitin specific protease 18 (Usp18), mRNA	5.7
25	NM_015783	interferon-stimulated protein (15 kDa) (Isg15), mRNA	5.6
26	NG_001413.1	midkine pseudogene 1 (Mdk-ps1) on chromosome 11	5.6
27	NM_008538	myristoylated alanine rich protein kinase C substrate (Macs), mRNA	5.4
28	NM_016754	myosin light chain, phosphorylatable, fast skeletal muscle (Mylpf), mRNA	5.2
29	NM_007792	cysteine-rich protein 2 (Csrp2), mRNA	5.2
30	NM_010501	interferon-induced protein with tetratricopeptide repeats 3 (Ifit3), mRNA	5.1

Top 30 up- or down-regulated genes under semi-confluent culture condition. Red- or green-heighlighted genes are those that were commonly expressed between QRsPIR-1 and QRsPIR-5 in comparison with the parental QRsP.

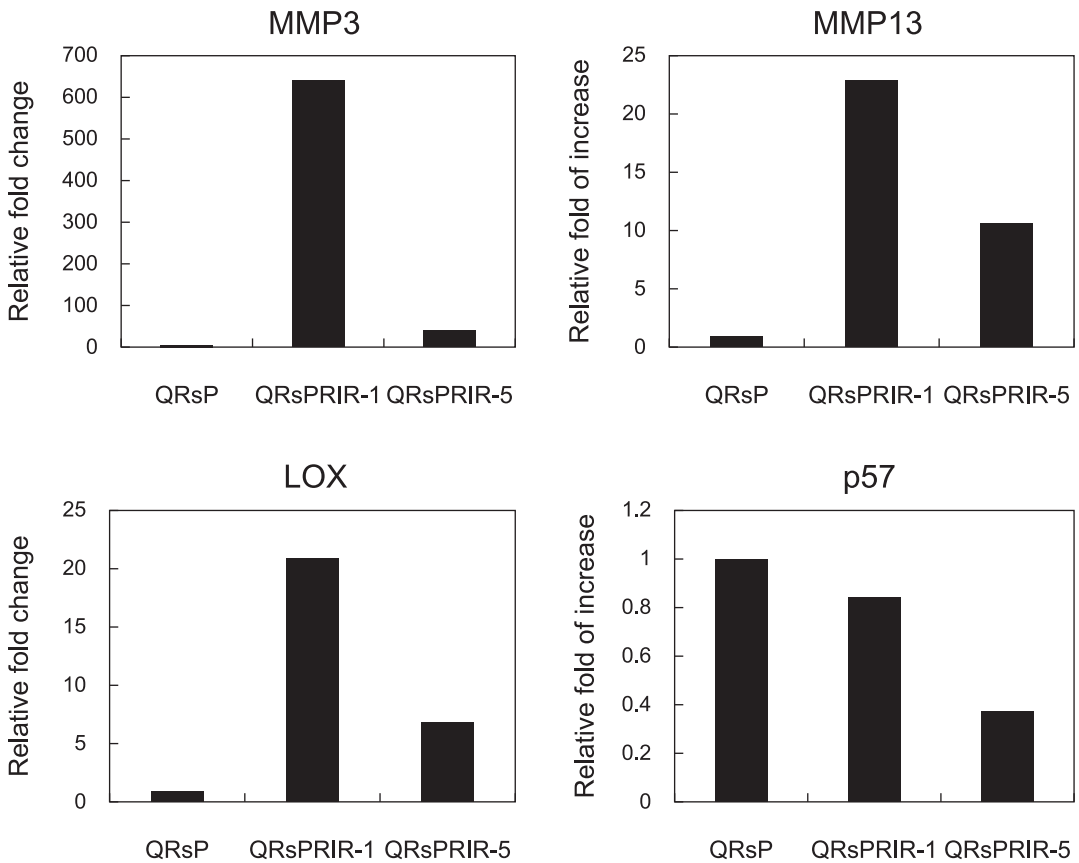

Fig. 1. Results of real-time RTPCR for p57, MMP3, MMP13, and LOX are shown. Note that the genes that are associated with invasiveness (MMP3, MMP13, and LOX) are strongly expressed.

Does a certain percentage of cells survive just by chance or because those cells had a tolerant genetic profile in the first place (i.e., tolerant cell selection)? If selection is the case, are surviving cells like cancer stem cells (Gilbert and Ross, 2009)? Addressing these issues will help us better understand tumor kinetics during radiotherapy and could provide us with new insights towards the development of novel therapies.

Materials and Methods

Cell culture and colony assay

QRsP transplantable fibrosarcoma cells, p53 wild type, (Okada *et al.*, 1992), were cultured in 8% FBS containing DMEM. Ninety percent confluent QRsP cells were irradiated at a dose of 10 Gy using a Cobalt system (Toshiba, Japan). The dose rate was kept at 1.8 Gy/min, and the distance from the source to the mice was 80 cm. One hour post irradiation, 1×10^4 of trypsinized QRsP cells were seeded on 35 mm culture dishes. At the same time, 100 non-irradiated QRsP cells were also seeded on 35 mm culture dishes to confirm plating efficiency. These cells were cultured for 10 days with DMEM followed by methanol fixation and Giemsa staining.

Cell cloning

QRsP cells irradiated at a dose of 10 Gy were seeded onto 10 cm dishes and cultured for 14 days. Well-demarcated colonies were trypsinized using a cloning cylinder and grown in DMEM. Six independent cell lines were established and named QRsPIR-1 through QRsPIR-6. A subset of these cells was irradiated at a dose of 10 Gy and 1×10^4 of trypsinized cells were cultured for 10 days, and the number of methanol-fixed and Giemsa-stained colonies were counted. The rest of the cells were stored at –80°C for future experiments.

DNA microarray analysis

For *in vitro* comparison, total RNA was extracted from semi-confluent QRsP parental cells and QRsPIR-1 cells. A comparison also made for the parental cells and QRsP-5 cells. We also prepared RNA from both QRsP- and QRsPIR-1-derived tumors (one animal each). Extracted RNA was labeled and hybridized onto a mouse microarray chip, followed by signal detection and computer analysis according to the manufacturer's protocol (Agilent Technologies,

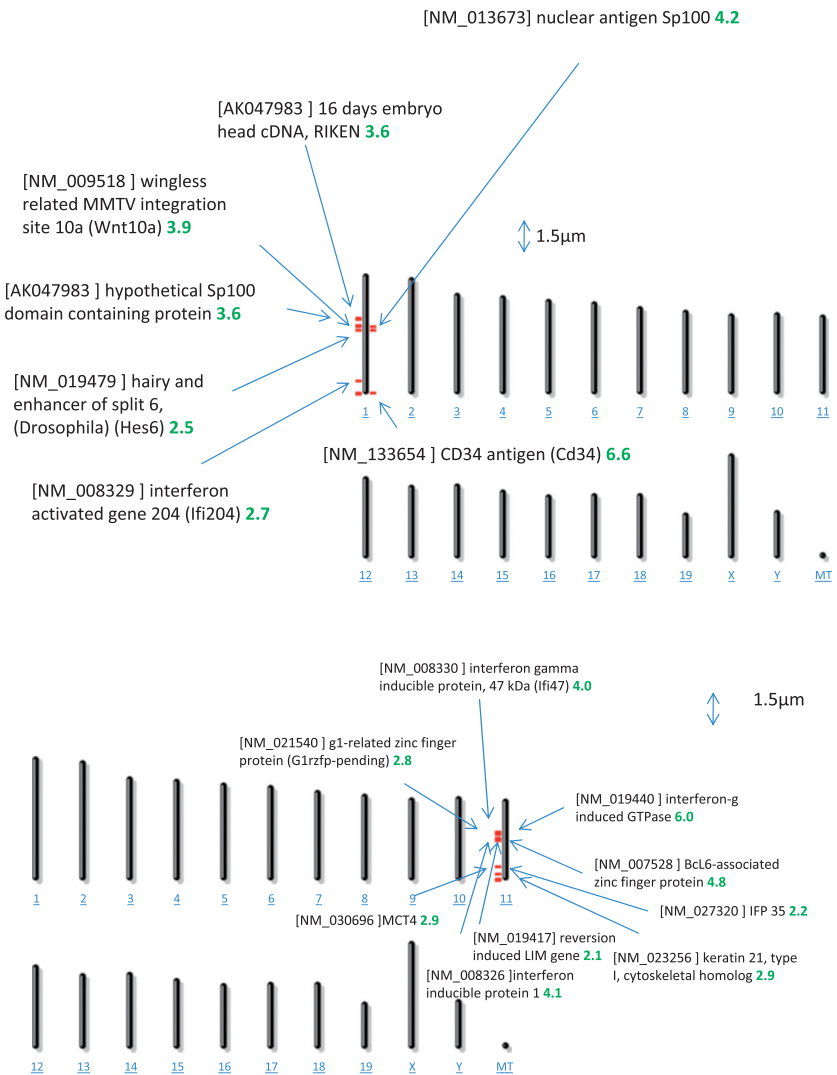

Fig. 2. The loci of genes that are down-regulated for GRsPIR-1 on chromosome 1 and 11. There are two regions that could be within a "target volume" of ionizing irradiation. The target volume can be translated into a cube of 1.5 µm on each side (arrow). Numbers highlighted in green indicate fold changes.

Santa Clara, CA). Genes up- or down-regulated more than 2 fold are summarized in tables (hereafter referred to as "array results"). NCBI Map Viewer was used to locate the genes on chromosomes.

Cell implantation and histopathology

Semi-confluent QRsP parent cells and QRsPIR-1 cells were trypsinized and resuspended in PBS. One thousand PBS-suspended cells were injected subcutaneously into the dorsal side of 6-week-old female C57BL/6 mice (5 animals each). On the 28th day, all animals were sacrificed and the tumor masses were dissected. The experiments strictly followed the animal care guidelines of Hokkaido University. Tumor tissues were fixed with 10% formaldehyde and embedded in paraffin according to routine pathological procedures. A 5 micrometer-thick section of each specimen was stained with hematoxylin and eosin. Two pathologists independently examined the samples. Mitotic cells were counted in five randomly selected on high-power fields, and the average numbers of mitoses were obtained.

Real-time PCR

Total RNA was extracted from QRsP parental cells, QRsPIR-1 and QRsPIR-5 cells using the Isogen RNA extraction kit (Nippon Gene) according to the manufacturer's instructions. cDNA was prepared from the total RNA with a reverse transcriptase (Invitrogen), oligo dT and dNTP mixture (Promega). The indicated cDNA was specifically amplified by thermal cycler (LightCycler; Roche Applied Science, Indianapolis, IN) using the corresponding primer pairs and probes for mouse MMP3, MMP13, LOX, p57 and β-actin. The following primers were used: MMP-3: sense, 5'-TTGTTCTT-TGATGCAGTCAGC-3'; anti-sense, 5'-GATTTGCGCCAAAA-

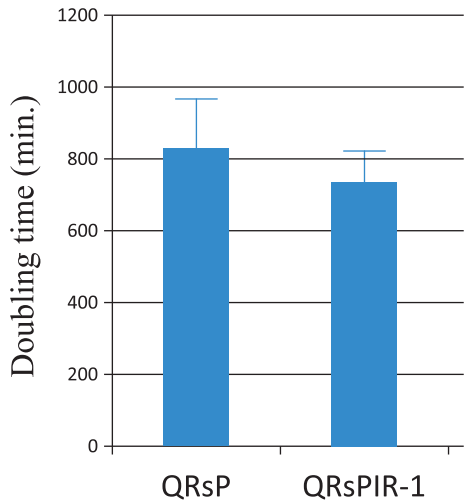

Fig. 3. Average and standard deviations of cell cycle time are as follows: 831.8+/–180.7 min for QRsP and 738.3+/–72.7 min for QRsPIR-1 ($p<0.05$, Student's *t*-test).

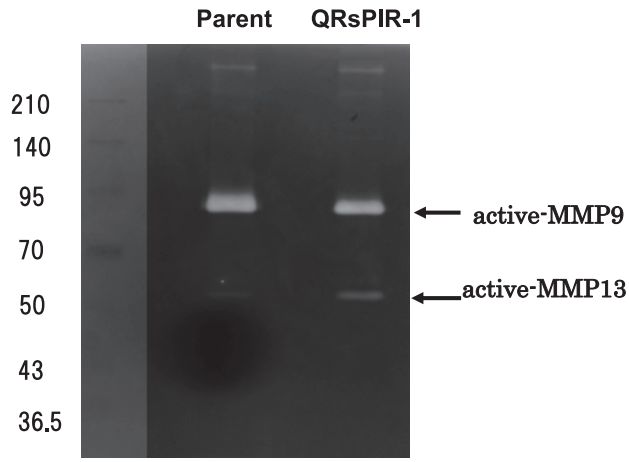

Fig. 4. Collagen zymography. A band corresponding to MMP13 is observed.

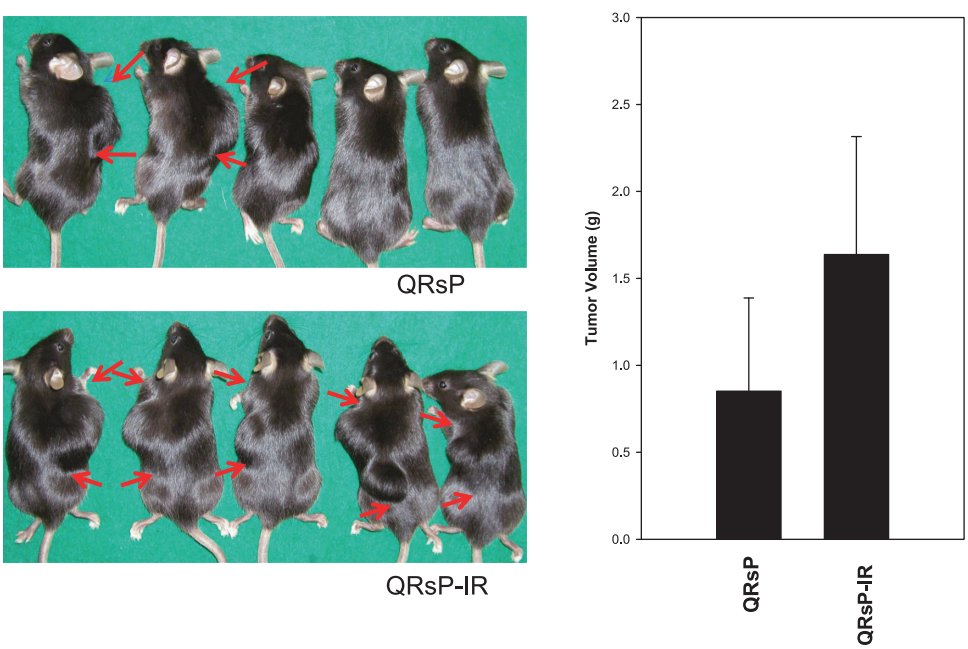

Fig. 5. QRsP or QRsPIR-1 cells (1×10^4 cells) were implanted. All animals implanted with QRsPIR-1 cells showed a palpable tumor mass, whereas 3 out of 5 animals implanted with QRsP parent cells had no signs of tumor. The average weights of the dissected tumor masses were plotted. The volumes of the QRsPIR-1-derived tumor masses were larger than the QRsP tumor masses, but the difference was not statistically significant.

GTGC-3'; MMP13: sense, 5'-GCCAGAACTTCCCAACCAT-3'; anti-sense, 5'-TCAGAGCCCAGAATTTTCTCC-3'; LOX: sense, 5'-CAGGCTGCACAATTTCACC-3'; anti-sense, 5'-CAAACAC-CAGGTACGGCTTT-3'; p57: sense, 5'-CAGGACGAGAATCA-AGAGCA-3'; anti-sense, 5'-GCTTGGCGAAGAAGTCGT-3'; and β-actin: sense, 5'-AAGGCCAACCGTGAAAAGAT-3'; GTGGT-ACGACCAGAGGCATAC-3'.

Results and Discussion

QRsP is a transplantable fibrosarcoma-cell-line derived from C57BL/6 mice (Kobayashi *et al.*, 2002). This gave us an advantage over the usual nude mouse experiments in the sense that "host vs. tumor" reactions are occurring. On culture condition, 28 out of 1×10^4 QRsP cells survived 10 Gy

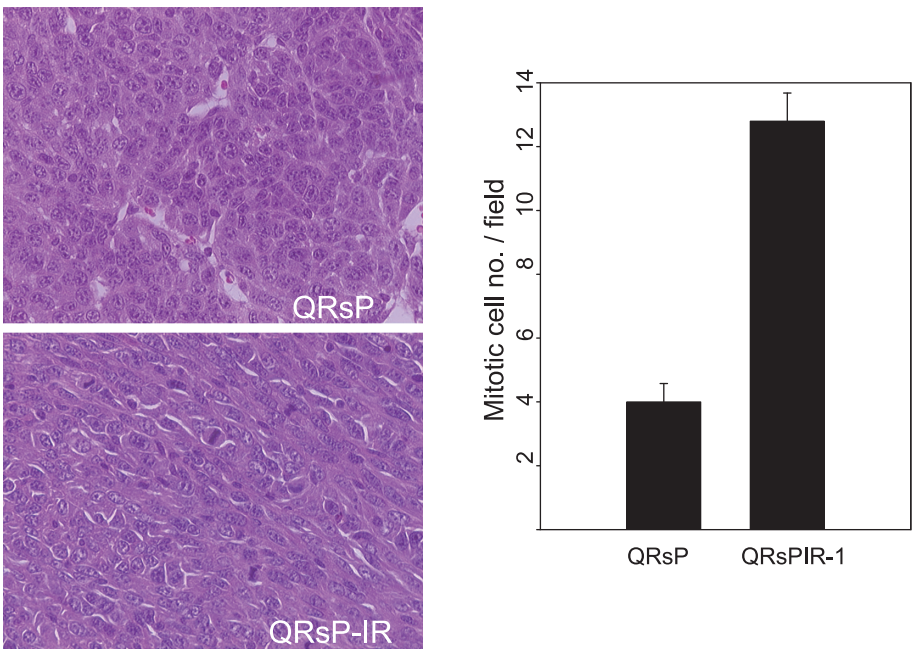

Fig. 6. Histopathological features of the tumors are indicated. Both QRsP and QRsPIR-1 tumors showed the same histological features despite different mitotic cell number. A significant difference in the number of mitosis per high-power field was observed.

irradiation and made well-demarcated colonies. This figure is comparable to other sarcoma cell lines (Kranjc *et al.*, 2005). The results of cDNA analyses are shown in Table 1a and b, in which the top 30 genes are listed in the order of the fold magnitude for QRsPIR-1. Highlighted genes by red or green suggest genes up- or down-regulated for QRsPIR-5 as well. Seven (23%) or 15 (50%) genes are commonly up- or down-regulated between QRsPIR-1 and QRsPIR-5. If we set 2.0-fold as a threshold, 132 or 238 genes were up- or down-regulated for QRsPIR-1. Among these genes, 11 (8.3%) or 63 (26.5%) genes were commonly up- or down-regulated respectively, between QRsPIR-1 and QRsPIR-5. The gene expression levels of MMP3, MMP13, LOX, and p57 were further evaluated by quantitative real-time RT-PCR. As shown in Fig. 1, MMP3, MMP13, and LOX were up-regulated (643.6-, 22.9-, and 20.8-fold for QRsPIR-1, 40.2-, 10.6-, and 6.9-fold for QRsPIR-5, respectively). p57 was down-regulated 0.8-fold for QRsPIR-1, 0.3-fold for QRsPIR-5,respectively. These data were quite consistent with our array results except for p16, for which real-time PCR gave us neither positive nor negative data for some unknown reasons. The fact that our commonly down-regulated genes outnumbered up-regulated ones is probably explained by DNA damage by irradiation, which, in nature, means the "destruction" of genes. There was an interesting finding that came out from the Monte Carlo simulation (Date and Shimozuma, 2001) suggesting that genes prone to irradiation are not uniformly separated on chromosomes but presumably are located within a particular "target volume" as described below. Such a target has a volume of 3.2 μm^3 (a cube of 1.47 μm on each side), in which radicals (i.e. -OH, ·OH, etc.) make a cluster (Date, in preparation). An example of the assumption is shown in Fig. 2a and b, in which 7 out of 7 down-regulated genes on chromosome 1 are located in two separate "target volumes", and 8 out of 9 down-regulated genes on chromosome 11 in two such volumes. It is interesting that cyclin-dependent kinase inhibitors (CDKIs), p16/INK4A and p57/Kip2, were particularly down-regulated in QRsPIR-1 cells (14.8- and 12.0-fold, respectively). CDKIs are keys to regulate cell cycle (Le *et al.*, 2010). Indeed, cell doubling time measured under phase contrast microscopy at five min intervals was shorter for QRsPIR-1 (Fig. 3). p16 is also known to cause radiation-induced premature senescence (Rodier *et al.*, 2009; Muthna *et al.*, 2010). On the side of up-regulated genes, the following genes caught our attention: matrix proteinase (MMP) 13 and 3 (25.8- and 22.5-fold), lysl oxidase (LOX, 4.8-fold), and integrin beta 7 (3.4-fold). MMPs and LOX are highly associated with the invasive nature of malignant tumors (Zhang *et al.*, 2010; Brekhman and Neufeld, 2009). Integrin beta 7 is also a key molecule of cancer cell adhesion and invasion (Kielosto *et al.*, 2009). To verify the invasive activity of MMPs, a collagen zymography was performed and a band probably corresponding to MMP13 was detected (Fig. 4). These data encouraged us to proceed to *in vivo* study. Upon macroscopic examination on day 28 after tumor implantation, 2 mice out of 5 that were implanted with QRsP parental cells demonstrated a palpable tumor

Table II.

	Gene Name	Description	Fold Change
(a) Up-regulated genes *in vivo*			
1	NM_021443	small inducible cytokine A8 (Scya8), mRNA	26.1
2	NM_009890	cholesterol 25-hydroxylase (Ch25h), mRNA	18.0
3	NM_011331	small inducible cytokine A12 (Scya12), mRNA	16.2
4	NM_133237	ethanol induced gene product EIG180 (EIG180), mRNA	11.5
5	NM_133775	RIKEN cDNA 9230117N10 gene (9230117N10Rik), mRNA	11.4
6	AK010014	similar to ALPHA-INTERFERON INDUCIBLE PROTEIN (FRAGMENT) [Mesocricetus auratus]	10.9
7	NM_030707	macrophage scavenger receptor 2 (Msr2), mRNA	9.9
8	NM_009153	sema domain, immunoglobulin domain (Ig), short basic domain, secreted, (semaphorin) 3B (Sema3b), mRNA	9.4
9	BC004738	Similar to dual specificity phosphatase 9, clone MGC:6681 IMAGE:3501447, mRNA, complete cds	9.0
10	NM_009849	ectonucleoside triphosphate diphosphohydrolase 2 (Entpd2), mRNA	9.0
11	S78079	scleraxis=basic helix-loop-helix transcription factor [mice, embryos, mRNA, 1140 nt]	9.0
12	NM_024474	Emu2 gene (Emu2-pending), mRNA	8.4
13	AK028122	GTP CYCLOHYDROLASE I FEEDBACK REGULATORY PROTEIN homolog [Rattus norvegicus]	8.4
14	AK034430	CALCIUM-INDEPENDENT ALPHA-LATROTOXIN RECEPTOR 2 PRECURSOR (LATROPHILIN 2) (LRP2) (CIRL) (CL2) (LPH2) homolog [Rattus norvegicus]	8.3
15	BC022666	MICROFIBRIL-ASSOCIATED GLYCOPROTEIN 4 homolog [Homo sapiens]	7.8
16	AK004161	unclassifiable	7.4
17	AF349658	T-box 1 transcription factor (Tbx1) mRNA, complete cds	7.3
18	AK047877	dJ667H12.2.1 (novel protein (isoform 1)) {Homo sapiens}	6.8
19	NM_021365	X-linked lymphocyte-regulated 4 (Xlr4), mRNA	6.7
20	NM_008599	small inducible cytokine B subfamily (Cys-X-Cys), member 9 (Scyb9), mRNA	6.1
21	NM_138683	thrombospondin type 1 domain (R-spondin), mRNA	6.0
22	AK008765	retinol binding protein 4, plasma	5.9
23	NM_133804	expressed sequence R74613 (R74613), mRNA	5.9
24	BC022157	clone IMAGE:5134400, mRNA, partial cds	5.9
25	AK029490	DJ977B1.4.1 (ISOFORM 1) (TGIF2) (TGFB-INDUCED FACTOR 2) (TALE FAMILY HOMEOBOX) homolog [Homo sapiens]	5.8
26	NM_007993	fibrillin 1 (Fbn1), mRNA	5.6
27	AK077362	hypothetical protein	5.6
28	AK014074	hypothetical AAA ATPase superfamily containing protein	5.6
29	AK012857	LEUKOCYTE SURFACE	5.5
30	AK028246	lymphoid enhancer binding factor 1	5.4
(b) Down-regulated genes *in vivo*			
1	NM_010217	connective tissue growth factor (Ctgf), mRNA	31.3
2	NM_008471	keratin complex 1, acidic, gene 19 (Krt1-19), mRNA	31.2
3	AB041591	brain cDNA, clone MNCb-2717	27.4
4	AK005747	RIKEN cDNA 1700007P19 gene	25.2
5	NM_023256	keratin 21, type I, cytoskeletal homolog [Rattus norvegicus]	25.2
6	NM_021400	proteoglycan 3 (megakaryocyte stimulating factor, articular superficial zone protein) (Prg4), mRNA	24.2
7	BC009120	matrix gamma-carboxyglutamate (gla) protein	22.4
8	AK042546	PROTOCADHERIN PRECURSOR PCDH	19.8
9	NM_007833	decorin (Dcn), mRNA	19.4
10	AK019470	similar to UDP-N-ACETYL-ALPHA-D-GALACTOSAMINE:POLYPEPTIDE N-ACETYLGALACTOSAMINYLTRANSFERASE 7 [Homo sapiens]	18.5
11	NM_007679	CCAAT/enhancer binding protein (C/EBP), delta (Cebpd), mRNA	17.8
12	NM_013743	pyruvate dehydrogenase kinase 4 (Pdk4), mRNA	13.9
13	BC004710	ADAPTOR MOLECULE SRCASM	12.9
14	NM_013602	metallothionein 1 (Mt1), mRNA	12.2
15	NM_010638	Kruppel-like factor 9 (Klf9), mRNA	12.2
16	NM_013492	clusterin (Clu), mRNA	11.2
17	NM_022315	secreted modular calcium binding protein 2 (Smoc2), mRNA	11.1
18	NM_011315	serum amyloid A 3 (Saa3), mRNA	10.9
19	NM_013864	N-myc downstream regulated 2 (Ndr2), mRNA	10.8
20	NM_010052	delta-like 1 homolog (Drosophila) (Dlk1), mRNA	10.5
21	NM_007428	angiotensinogen (Agt), mRNA	9.9
22	AK009928	unknown EST	9.6
23	NM_133753	RIKEN cDNA 1300002F13 gene (1300002F13Rik), mRNA	9.4
24	NM_008008	fibroblast growth factor 7 (Fgf7), mRNA	8.8
25	NM_019707	cadherin 13 (Cdh13), mRNA	8.6
26	NM_023122	glycoprotein m6b (Gpm6b), mRNA	8.3
27	NM_011198	prostaglandin-endoperoxide synthase 2 (Ptgs2), mRNA	7.7
28	BC027543	FAT CELL SPECIFIC LOW MOLECULAR WEIGHT PROTEIN	7.7
29	NM_011361	serum/glucocorticoid regulated kinase (Sgk), mRNA	7.6
30	NM_009166	sorbin and SH3 domain containing 1 (Sorbs1), mRNA	7.3

Top 30 up- or down-regulated genes from the QRsPIR-1-derived tumor. Highlighted genes are those seen in Table 1 (i.e., up- or down-regulated genes in QRsPIR-1 *in vitro*)

mass whereas all 5 mice implanted with QRsPIR-1 cells developed obvious tumors. The average size of the tumor mass derived from QRsPIR-1 cells was larger than that of those derived from QRsP parental cells (Fig. 5). Two out of five (40%) QRsPIR-1 tumor showed muscular invasion while no QRsP-derived tumors showed any invasion to the surrounding tissues. Under histopathological examination, QRsP parental and QRsSPIR-1-derived tumor tissue showed the same morphological features (Fig. 6). However, QRsPIR-1-derived tumor tissue showed frequent cell mitoses. The mean mitotic cell number was 4.0+/–3.9(SD) for QRsP, and 12.8+/–3.4 for QRsPIR-1 (Fig. 5; $p<0.01$, Student's *t*-test). These *in vivo* results clearly demonstrated that QRsPIR-1 cells have an aggressive nature compared with the parental QRsP cells, and reflected the results of cDNA analyses. One of the limitations of the present study may be too much emphasis on cDNA analyses. A living creature, a collection of cells, is always in a dynamic state, therefore its mRNA expression can change as a function of a given environment. This implies the data presented here might have been different if sampled even a few minutes earlier or later. A typical example is cDNA data obtained from QRsPIR-1-derived tumor tissue. The array results was significantly different from the *in vitro* one (Table 2a and b). Several cell-cycle related genes were up-regulated: cyclin A2 (2.5-fold), cyclin B2 (2.2-fold), and PCNA (2.3-fold). Angiogenesis-related genes were also up-regulated: T-box 1 transcription factor (7.3-fold) (Kobayashi *et al.*, 2002) and PDGF (2.5-fold) (Kumar *et al.*, 2010). Interestingly, one of the cancer stem cell markers, CD34 (Pierce *et al.*, 2008), was up-regulated (4.0-fold). One might think of normal tissue involvement for these up-regulated genes. The pathologists are fully experienced in handling tumor sampling, and we believe the array results came mostly from the tumor tissues.

In conclusion, irradiation is an effective tool for cancer treatment; however, if tumor cells survive ionizing irradiation, those cells may be more aggressive (i.e., rapid proliferation and higher invasiveness). The higher transplantation ratio might be indicative of the presence of cancer stem cell in the QRsPIR-1-derived tumor, though the up-regulation of CD34 alone is not enough to support the notion.

Acknowledgments. This study was supported in part by a Grant-in-Aid for Scienific Research (B20390319) provided by the Ministry of Education, Culture, Sports, Science and Technology of Japan. We wish to thank Dr. Futoshi Okada (Department of Biochemistry and Molecular Biology, Yamagata University Graduate School of Medical Science, Yamagata, Japan) for providing us with the QRsP cells used in this research and Mr. Neil Colley for his kind assistance in manuscript preparation.

References

Bernier, J. 2005. Alteration of radiotherapy fractionation and concurrent chemotherapy: a new frontier in head and neck oncology? *Nat. Clin. Pract. Oncol.*, **2**: 305–314.

Brekhman, V. and Neufeld, G. 2009. A novel asymmetric 3D *in vitro* assay for the study of tumor cell invasion. *BMC Cancer*, **30**: 415–426.

Date, H. An Interpretation of the Linear Quadratic Relation for Cell Surviving Fraction in Radiation Exposure. *Int. J. Radiat. Biol.*, in preparation.

Date, H. and Shimozuma M. 2001. Boltzmann equation description transport in an electrical field with cylindrical symmetry. *Phys. Rev. E. Strat. Nonlin. Soft Matter Phys*., **64**: 664101–664108.

Gilbert, C.A. and Ross, A.H. 2009. Cancer stem cells: cell culture, markers, and targets for new therapies. *J. Cell. Biochem.*, **108**: 1031–1038.

Inoue, T., Shimizu, S., Onimaru, R., Takeda, A., Onishi, H., Nagata, Y., Kimura, T., Karasawa, K., Arimoto, T., Hareyama, M., Kikuchi, E., and Shirato, H. 2009. Clinical outcomes of stereotactic body radiotherapy for small lung lesions clinically diagnosed as primary lung cancer on radiologic examination. *Int. J. Radiat. Oncol. Biol. Phys*., **75**: 683–687.

Kielosto, M., Nummela, P., Jarvinen, K., Yin, M., and Holtta, E. 2009. Identification of integrins alpha6 and beta7 as c-Jun- and transformation-relevant genes in highly invasive fibrosarcoma cells. *Int. J. Cancer*, **125**: 1065–1073.

Kim, J.J. and Tannock, I.F. 2005. Repopulation of cancer cells during therapy: an important cause of treatment failure. *Nat. Rev. Cancer*, **5**: 516–525.

Kobayashi, T., Okada, F., Fujii, N., Tomita, N., Ito, S., Tazawa, H., Aoyama, T., Choi, S.K., Shibata, T., Fujita, H., and Hosokawa, M. 2002. Thymosin-beta4 regulates motility and metastasis of malignant mouse fibrosarcoma cells. *Am. J. Pathol*., **160**: 869–882.

Kranjc, S., Cemazar, M., Grosel, A., Sentjurc, M., and Sersa, G. 2005. Radiosensitising effect of electrochemotherapy with bleomycin in LPB sarcoma cells and tumors in mice. *BMC Cancer*, **5**: 115.

Kumar, A., Hou, X., Lee, C., Li, Y., Maminishkis, A., Tang, Z., Zhang, F., Langer, H.F., Arjunan, P., Dong, L., Wu, Z., Zhu, L.Y., Wang, L., Min, W., Colosi, P., Chavakis, T., and Li, X. 2010. Platelet-derived growth factor-DD targeting arrests pathological angiogenesis by modulating glycogen synthase kinase-3beta phosphorylation. *J. Biol. Chem.*, **285**: 15500–15510.

Le, O.N., Rodier, F., Fontaine, F., Coppe, J.P., Campisi, J., DeGregori, J., Laverdière, C., Kokta, V., Haddad, E., and Beauséjour, C.M. 2010. Ionizing radiation-induced long-term expression of senescence markers in mice is independent of p53 and immune status. *Aging Cell*, **9**: 398–409.

Muthna, D., Soukup, T., Jirina, V., Mokry, J., Cmielova, J., Visek, B., Jiroutova, A., Havelek, R., Suchanek, J., Filip, S., English, D., and Rezacova, M. 2010. Irradiation of Adult Human Dental Pulp Stem Cells Provokes Activation of p53, Cell Cycle Arrest and Senescence but not Apoptosis. *Stem Cells Dev.*, in press.

Okada, F., Hosokawa, M., Hamada, J.L., Hasegawa, J., Kato, M., Mizutani, M., Ren, J., Takeichi, N., and Kobayashi, H. 1992. Malignant progression of a mouse fibrosarcoma by host cells reactive to a foreign body. *Br. J. Cancer*, **66**: 635–639.

Pierce, A., Barron, N., Linehan, R., Ryan, E., O'Driscoll, L., Daly, C., and Clynes, M. 2008. Identification of a novel, functional role for S100A13 in invasive lung cancer cell lines. *Eur. J. Cancer*, **44**: 151–159.

Rodier, F., Coppé, J.P., Patil, C.K., Hoeijmakers, W.A., Muñoz, D.P., Raza, S.R., Freund, A., Campeau, E., Davalos, A.R., and Campisi, J. 2009. Persistent DNA damage signalling triggers senescence-associated inflammatory cytokine secretion. *Nat. Cell Biol.*, **11**: 973–979.

Zhang, Y., Gong, L.H., Zhang, H.Q., Du, Q., You, J.F., Tian, X.X., and Fang, W.G. 2010. Extracellular ATP enhances *in vitro* invasion of prostate cancer cells by activating Rho GTPase and upregulating MMPs expression. *Cancer Lett.*, **28**: 189–197.

(Received for publication, July 1, 2010, accepted, September 3, 2010 and published online, December 25, 2010)